

ISSN 1678-3921

Journal homepage: www.embrapa.br/pab

For manuscript submission and journal contents,
access: www.scielo.br/pab







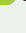
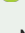
Probabilistic analysis of vulnerability to stenospermocarpy due to hygrothermal stress in 'Palmer' mangoes using a copula-based approach

Abstract – The objective of this work was to probabilistically identify susceptible seasons to the highest incidence of stenospermocarpic fruit in 'Palmer' mangoes, using univariate and copula procedures. Additionally, the impact of climatic variables on price fluctuations in the mango market was evaluated in the region of the Vale do Submédio São Francisco, Brazil. The normal, log-normal, gamma, and generalized extreme value distributions, as well as the Frank copula, were fitted to temperature and relative humidity data (2007–2018) obtained from the meteorological station of Universidade do Estado da Bahia. The adequacy of the distributions was verified using the Kolmogorov-Smirnov, Cramér-von Mises, and Anderson-Darling tests. The Frank copula is suitable for the joint modeling of the maximum temperature and minimum relative humidity. The occurrence of high temperatures and low relative humidity affects the price of mangoes. November shows a high probability of the simultaneous occurrences of high temperatures and low relative air humidity, which makes 'Palmer' mango orchards in full bloom (or early fruiting) significantly subject to extreme weather conditions that favor higher rates of stenospermocarpy in the harvests from April to May.

Index terms: *Mangifera indica*, mango market, weather influence.

Análise probabilística da vulnerabilidade à estenospermocarpia por estresse higratérmico em mangas 'Palmer', por meio de abordagem baseada em cópulas

Resumo – O objetivo deste trabalho foi identificar, de forma probabilística, as épocas suscetíveis à maior incidência de frutos estenospermocárpicos em mangas 'Palmer', por meio de procedimentos univariados e de cópulas. Além disso, o impacto de variáveis climáticas sobre a oscilação de preços no mercado da manga foi avaliado na região do Vale do Submédio São Francisco, Brasil. As distribuições normal, log-normal, gama e generalizada de valores extremos, bem como a cópula de Frank, foram ajustadas aos dados de temperatura e umidade relativa (2007–2018), obtidos na estação meteorológica da Universidade do Estado da Bahia. A adequação das distribuições foi verificada por meio dos testes de Kolmogorov-Smirnov, Cramér-von Mises e Anderson-Darling. A cópula de Frank é adequada para modelar, conjuntamente, a temperatura máxima e a umidade relativa mínima do ar. As ocorrências de altas temperaturas e baixa umidade relativa afetam os preços de mangas. Novembro apresenta grande probabilidade da ocorrência

Edgo Jackson Pinto Santiago⁽¹⁾ ,
José Ramon Barros Cantalice⁽²⁾ ,
Frank Gomes-Silva⁽²⁾ ,
Maria Aparecida do Carmo Mouco⁽³⁾ ,
Antonio Samuel Alves da Silva⁽²⁾ ,
Moacyr Cunha Filho⁽²⁾ ,
Gertrudes Macario de Oliveira⁽⁴⁾ ,
Ana Karla da Silva Freire⁽⁵⁾ 

⁽¹⁾ Universidade de Pernambuco, Núcleo Comum das Licenciaturas do Campus Petrolina, BR 203, KM 2, s/nº, Vila Eduardo, CEP 56328-900 Petrolina, PE, Brazil. E-mail: edgojps@gmail.com

⁽²⁾ Universidade Federal Rural de Pernambuco, Departamento de Estatística e Informática, Rua Dom Manuel de Medeiros, s/nº, Dois Irmãos, CEP 52171-900 Recife, PE, Brazil. E-mail: ramoncanta21@gmail.com, franksinatrags@gmail.com, samuemathematical@gmail.com, moacyr.cunhafo@ufrpe.br

⁽³⁾ Embrapa Semiárido, BR 428, Km 152, Zona Rural, Caixa Postal 23, CEP 56302-970 Petrolina, PE, Brazil. E-mail: mariamouco@msn.com

⁽⁴⁾ Universidade do Estado da Bahia, Departamento de Tecnologia e Ciências Sociais, Campus III, Rua Edgar Chastinet, s/nº, São Geraldo, CEP 48905-680 Juazeiro, BA, Brazil. E-mail: gmacariodeoliveira@yahoo.com.br

⁽⁵⁾ Universidade Federal Rural de Pernambuco, Núcleo de Assistência e Promoção à Saúde, Rua Cento e Sessenta e Três, nº 300, Garapu, CEP 54503-900 Cabo de Santo Agostinho, PE, Brazil. E-mail: akarlasf@hotmail.com

 Corresponding author

Received

July 23, 2023

Accepted

January 11, 2024

How to cite

SANTIAGO, E.J.P.; CANTALICE, J.R.B.; GOMES-SILVA, F.; MOUÇO, M.A. do C.; SILVA, A.S.A. da; CUNHA FILHO, M.; OLIVEIRA, G.M. de; FREIRE, A.K. da S. Probabilistic analysis of vulnerability to stenospermocarpny due to hygrothermal stress in 'Palmer' mangoes using a copula-based approach. **Pesquisa Agropecuária Brasileira**, v.59, e03467, 2024. DOI: <https://doi.org/10.1590/S1678-3921.pab2024.v59.03467>.

simultânea de altas temperaturas e baixa umidade relativa do ar, o que torna os pomares de manga 'Palmer' em plena floração (ou frutificação precoce) significativamente sujeitos a condições climáticas extremas, que favorecem taxas mais elevadas de estenospermocarpia nas safras de abril a maio.

Termos para indexação: *Mangifera indica*, mercado de manga, influência do clima.

Introduction

The formation of stenospermocarpic fruit occurs due to the interruption of fertilized ovules, or when there are defects in endosperm development (Kaya et al., 2022) often caused by abnormal meiosis. In mangoes (*Mangifera indica* L.), although the mechanisms that trigger this entire process are uncertain, the occurrence of either high or low temperatures during flowering and/or beginning of fruiting are related to fruit that exhibit this anomaly.

Flowering is controlled by multiple and complex factors, both internal and environmental ones (Heide et al., 2020), such as thermal variation during different periods of the year. Therefore, the effect of temperature on flowering is one of the main factors influencing fruit production.

High temperatures accelerate and low temperatures delay the growth rate of the pollen tube, therefore these conditions also affect the pistil development speed (Thingreingam Irenaeus & Mitra, 2014). Thermal rise during flowering accelerates the pollen tube growth and maturation, thus contributing with stigma and

ovule degeneration (Beltrán et al., 2019; Montalt et al., 2019), which can reduce the effective pollination period, since ovule will likely have a short life span. Additionally, increased temperature during the reproductive phases might lead to meiosis chromosome irregularities.

Due to hygrothermal stress resulting from high temperatures, low air humidity, and from possibly other factors not yet explained, the incidence of stenospermocarpic fruit has increased in 'Palmer' mangoes in the Vale do Submédio São Francisco river, a semiarid Brazilian region. This stress has caused a sharp reduction in the mango production, due to the development of small, irregular-shaped fruit ("manguitos") of no commercial value.

Despite the increase of the area planted with 'Palmer' in the region, driven by the significant economic gain, its vulnerability to thermal elevation in a climate change scenario may compromise its cultivation and make it unfeasible.

Detailed studies on the effects of high temperature and low relative humidity on mango reproductive structures are still scarce, and could not find any of report of this kind for 'Palmer' mango. Therefore, a study on the occurrence of high temperatures, throughout the year, associated with low relative humidity, could be important for predicting extreme weather events that may be detrimental to mango flowering.

Therefore, the objective of this work was to probabilistically identify seasons susceptible to the highest incidence of stenospermocarpic fruit in 'Palmer' mangoes, simultaneously associated with high temperatures and low relative air humidity, using univariate and copula procedures. Additionally, the impact of these climatic variables on price fluctuations in the mango market was evaluated in the Vale do Submédio São Francisco river. The results should help farmers to choose between running the risk of synchronizing flowering with less favorable seasons to flowering, while expecting higher product value in the market, or avoiding critical seasons by advancing or delaying flowering, being aware of management and production hindrances that might stem from these periods.

Materials and Methods

Data (2007-2018) were obtained from the meteorological station (09°24'50" S, 40°30'10" W, at 368 m altitude) of the Universidade do Estado da Bahia, municipality of Juazeiro, in Bahia state, Brazil. The following daily variables were used: minimum air temperature (Tmin), mean air temperature (Tmean), maximum air temperature (Tmax), minimum relative air humidity (Hmin), mean relative air humidity (Hmean), and maximum relative air humidity (Hmax).

In order to check the effect on the price of 'Palmer' mangoes due to fluctuations in Tmax and Umin, a series of prices (2012-2019) from the commercialization of this product at the supply state center of Bahia (Central Estadual de Abastecimento, CEASA) was used. This series was obtained from the city supply services of Juazeiro and updated according to the national wide consumer price index (IPCA) of the Instituto Brasileiro de Geografia e Estatística (IBGE) for the inflation of February 2020. The Pearson's correlation was used in the analysis, using an error type I, at 5% probability.

Normal (N), log-normal (LN), gamma (G), and generalized extreme value (GEV) probability distribution models were adjusted, using the probability density functions represented by the following equations:

$$f(x) = \frac{1}{\sigma\sqrt{2\pi}} \exp\left[-\frac{1}{2}\left(\frac{x-\mu}{\sigma}\right)^2\right], -\infty < x < \infty, \sigma^2 > 0, -\infty < \mu < \infty;$$

$$f(x) = \frac{1}{x\sigma\sqrt{2\pi}} \exp\left[-\frac{1}{2}\left(\frac{\log x - \mu}{\sigma}\right)^2\right], x > 0, \sigma^2 > 0, -\infty < \mu < \infty;$$

$$f(x) = \frac{1}{\beta^\alpha \Gamma(\alpha)} x^{\alpha-1} \exp\left(-\frac{x}{\beta}\right), x > 0, \alpha > 0, \beta > 0;$$

$$f(x) = \frac{1}{\sigma} \left[1 + \xi \left(\frac{x-\mu}{\mu} \right) \right]^{-\left(\frac{1+\xi}{\xi}\right)} \exp\left\{ - \left[1 + \xi \left(\frac{x-\mu}{\mu} \right) \right]^{-\left(\frac{1}{\xi}\right)} \right\},$$

$-\infty < x < \mu - \sigma/\xi$ para $\xi < 0$; $\mu - \sigma/\xi < x < \infty$ para $\xi > 0$.

To dismiss the hypothesis of the presence of trends and other nonstationary components that could affect the probabilistic structure, a Portmanteau test for white noise was employed in the datasets. This test utilized the Ljung-Box statistic, which is a modified version of the Box-Pierce chi-square statistic, to assess whether each series of observations over time was random and

independent. Sufficient evidence emerged to assume the absence of significant correlation in all datasets. Thus, parameter estimates for each model were conducted using the maximum likelihood estimation method.

The adequacy of probability distributions was checked using the Kolmogorov-Smirnov (KS) adherence test, with a maximum type I error probability at 5%, as well as the modified statistics from the Cramér-von Mises (W*) and Anderson-Darling (A*) goodness-of-fit tests (Chen & Balakrishnan, 1995).

These tests are used to compare nested or nonnested models, as is the case with the models used in the present study. Actually, for a given variable, the lowest values of W* or A* statistics are the indication of the best probability distribution to model the referred variable. According to Badr (2019) KS, W*, and A* statistics are free from distributions and employed to determine how well a proposed continuous model adjusts to the data in the observed sample.

The root mean square error (RMSE) and the maximum absolute error (MAE) were obtained using the following expressions:

$$RMSE = \sqrt{\frac{\sum_{i=1}^n (x_{(i)} - y_{(i)})^2}{n - m}},$$

$$MAE = \max |x_{(i)} - y_{(i)}|,$$

where: $x_{(i)}$ is the value of observation order i of the original sample; $y_{(i)}$ is the value of observation order i of the random sample, generated by the corresponding distribution based on adjustments estimates from the original sample; n is sample size; m is the number of parameters of the referred probability distribution. RMSE and MAE equations were used by Zalina et al. (2002) to compare the quality of adjustment, and thus, to have one more indication of the best distribution for univariate estimates.

After that, for each month, the probability of occurrence of different thermal levels and relative air humidity values was estimated using the best-fit distribution for the month in question, according to W* statistics.

For bivariate estimates, Frank Archimedean copula (with marginals following GEV) was used, with joint density and cumulative functions given, respectively, by the following equations

$$f_c(t;h) = \frac{\alpha \exp\{\alpha(t+h)\} \{\exp(\alpha)-1\}}{\{\exp(\alpha) + \exp[\alpha(t+h)]\} - \exp(\alpha t) - \exp(\alpha h)}$$

and

$$F_c(t;h) = -\frac{1}{\alpha} \log \left\{ 1 + \frac{[\exp(-\alpha t) - 1][\exp(-\alpha h) - 1]}{\exp(-\alpha) - 1} \right\}$$

where: $\alpha \in \mathbb{R}^*$ represents the structure of the dependence between variables that comprise the marginal distributions, $t = F(T_{\max})$ and $h = F(H_{\min})$ with $0 \leq t \leq 1$ and $0 \leq h \leq 1$. In equations 7 and 8, $F(T_{\max})$ and $F(H_{\min})$ represent, respectively, the cumulative distribution of T_{\max} and H_{\min} .

Copula is a cumulative joint distribution function obtained from the combination of two or more marginal cumulative distributions, at a free scale and with a certain degree of dependence, used to model multifactorial random phenomena.

According to Wang et al. (2017), copulas might model nonlinear dependence between two or more dependent variables with different marginal distributions. However, the suitable choice of marginal distributions is essential to effectively describe the structure of dependence between the variables.

Finally, for each month, the probability of simultaneous occurrence of different levels of maximum temperature and minimum relative air humidity was estimated using the bivariate Frank copula. Meteorological data of 2019 were used to compare the bivariate T_{\max} and H_{\min} estimates which actually occurred.

Results and Discussion

The Kolmogorov-Smirnov adherence test showed that the N distribution had significant (Table 1) adherence in most months for T_{mean} , T_{min} , and T_{max} temperatures. The GEV distribution stood out among the other probabilistic models regarding T_{max} , as it showed a higher number of adherences throughout the months. The LN distribution fit well to T_{max} data in the colder months – May, June, and July (Table 1).

These results are in accordance with those observed by Reis et al. (2022), who concluded that to model maximum air temperatures, the GEV distribution is recommended for use in warmer months, while the LN distribution is suitable for colder months. Krueel et al. (2015) also concluded that the GEV distribution was

appropriate for describing a series of daily minimum and maximum air temperatures.

Overall, N, LN, and G distributions did not have significant adherences in most months for H_{mean} and H_{max} . Conversely, the GEV distribution showed a significant adherence in nearly all months for H_{mean} and in all months for H_{min} (Table 1). However, it did not provide enough evidence to accept the hypothesis that it could adequately represent empirical H_{max} distribution. This is due to the low rainfall regime (529 mm per year) in the study region (Brazilian semiarid region). Therefore, scarce records of high relative humidity in the historical series might have been insufficient to characterize extreme values, which is required to be well modeled by GEV because, according to Reis et al. (2022), the GEV distribution is widely used to model extreme data in environmental sciences. When these characteristics are not observed, this distribution may not accurately characterize the phenomenon being studied, rendering it unsuitable for modeling it.

Although KS test is quite frequently used, it is not very powerful in distribution tails. That is why it is important to consider other metrics, such as W^* and A^* , when comparing probabilistic models. Badr (2019) compared the power of KS, W^* , and A^* tests and showed that KS was the least powerful and that W^* was the most powerful tests.

All studied distributions were suitable for most variables in a given month, in at least one W^* (Table 2) or A^* (Table 3) of the good-of-fitness tests. Despite that, G and N distributions regarding H_{mean} , as well as all distributions related to H_{max} , did not perform satisfactorily. However, GEV distribution produced the lowest values of statistical W^* and A^* for H_{min} and T_{max} in most months, and it was more suitable to model these variables. Similarly, GEV was the distribution that generally produced the lowest RMSE and MAE estimates (Figure 1).

The RMSE and MAE are standard procedures to compare quantile estimates (Zalina et al., 2002). In the determination of maximum annual rainfalls in the state of Amapá, Brazil, Gumbel and GEV distributions were observed as good fit, while GEV was the best fit, with the lowest RMSE values (Back & Cadornin, 2020).

Univariate probability estimates associated with different levels of temperature and relative humidity are displayed (Figure 2); colors are more intense with

increased possibility, and the values appear in each matrix slot .

There is 77% probability of Tmax being higher than or equal to 33°C in November, and this temperature level is most likely observed during this month (Figure 2 A). Additionally, there is a 42% chance of a Tmax equal to or higher than 35°C on 2.1 out of every 5 days. This month had extreme temperature values, which is much higher than the applicable limit for the mango reproductive phase. Issarakraisila & Considine (1994) defined the temperature range from 15°C to 33°C as ideal for pollen development in mangoes. Liu et al. (2023) observed that the optimal and maximum temperature ranges were 26.7–30.6°C and 30.4–34.3°C,

respectively, for pollen germination, and 27.9–32.1°C and 30.2–34.4°C, respectively, for pollen tube growth.

Thingreingam Irenaesus & Mitra (2014) explained that if temperatures higher than the optimal value occurs during the reproductive phase, the plant might experience a decreased pollen tube growth. Flowering mango trees outside the optimal temperature range may compromise the production levels. This has been frequently observed for 'Palmer' mango orchards in the region of the Vale do Submédio São Francisco river, especially in Petrolina and Juazeiro municipalities, which have reduced agricultural activity. Flowering in this region should occur from October to December for yield to be directed to the domestic market, in search of better prices and commercial windows. However, the

Table 1. Adherence of probability distribution functions to daily temperature (maximum, mean, and minimum air temperatures); relative humidity data (maximum, mean, and minimum relative air humidity), using the Kolmogorov-Smirnov test with a maximum type I error probability at 5% of the historical series from 2007 to 2018, in the municipality of Juazeiro, in the state of Bahia, Brazil.

Month	Tmean				Tmax				Tmin			
	N	LN	G	GEV	N	LN	G	GEV	N	LN	G	GEV
Jan.	*	*	*	—	*	ns	ns	*	*	*	*	*
Feb.	*	*	*	—	ns	ns	ns	*	*	*	*	*
Mar.	*	*	*	—	ns	ns	ns	*	*	*	*	*
Apr.	*	*	*	—	*	ns	ns	*	*	*	*	*
May	*	*	*	—	*	*	*	*	*	ns	ns	*
June	*	*	*	—	*	*	*	*	*	ns	ns	*
July	*	*	*	—	*	*	*	*	*	*	*	*
Aug.	*	*	*	*	*	ns	*	*	*	*	*	*
Sept.	*	*	*	*	*	ns	ns	*	*	*	*	—
Oct.	*	*	*	—	ns	ns	ns	ns	*	*	*	*
Nov.	*	ns	ns	—	ns	ns	ns	*	*	*	*	*
Dec.	ns	ns	ns	*	ns	ns	ns	*	*	*	*	*

Month	Hmean				Hmax				Hmin			
	N	LN	G	GEV	N	LN	G	GEV	N	LN	G	GEV
Jan.	ns	ns	ns	ns	ns	ns	ns	ns	ns	*	*	*
Feb.	ns	*	*	—	*	ns	*	ns	ns	*	*	*
Mar.	ns	ns	ns	—	ns	ns	ns	ns	ns	*	*	*
Apr.	ns	*	*	*	ns	ns	ns	ns	ns	*	ns	*
May	ns	*	*	*	ns	*	ns	*	*	*	*	*
June	ns	ns	ns	*	ns	ns	ns	*	ns	*	*	*
July	ns	ns	ns	*	ns	*	ns	*	ns	*	*	*
Aug.	ns	*	ns	*	ns	ns	ns	*	*	*	*	*
Sept.	ns	*	ns	*	ns	ns	ns	*	ns	*	*	*
Oct.	ns	ns	ns	*	ns	ns	ns	ns	ns	*	ns	*
Nov.	ns	ns	ns	*	ns	ns	ns	*	ns	*	*	*
Dec.	ns	ns	ns	*	ns	ns	ns	ns	ns	*	ns	*

Probability distribution models: N, normal; LN, log-normal; G, gamma; and GEV, generalized extreme value. Tmin, minimum air temperature; Tmean, mean air temperature; Tmax, maximum air temperature; Hmin, minimum relative air humidity; Hmean, mean relative air humidity; and Hmax, maximum relative air humidity. (—) Represents the impossibility of estimating the model parameters using the maximum likelihood method, due to the occurrence of a discontinuous region in the calculation of the number of derivatives. *Significant adherence. nsNonsignificant adherence.

present study shows that this period is less favorable, as high temperatures ($> 33^{\circ}\text{C}$) are more likely to occur.

Regarding, November had a 5% probability of relative air humidity – one out of every 20 days (Figure 2 D), with a daily Hmin lower than 20%. In addition, there was a 20% probability 1 out of every 5 days – of the daily Hmin ranging from 20 to 25% (which is very low). Low relative air humidity is detrimental to most plant species, especially during the reproductive phase, since it negatively affects flowering and fruiting. In mangoes, this condition might lead to an increased flower abortion rate and reduced fruit fixation, due to abscission caused by the endogenous increase in ethylene levels, in response to hygrothermal stress.

The highest probability (7%) of Tmean, equal to or exceeding 30°C , occurred in november (Figure 2 B). Although it is unlikely, but not impossible, the occurrence of this temperature level ($\geq 30^{\circ}\text{C}$) concurrently with the flowering of ‹Palmer› mango trees may impact the pollen formation. This happens because, according to Ramírez & Davenport (2010), high temperatures can reduce the pollen viability by up to 50%, potentially leading to the formation of stenospermocarpic fruits. This is particularly relevant when the mean temperature reaches at least 30°C because the maximum air temperature will have already reached extreme values. In addition, pollen is sensitive to temperature variations. These circumstances might affect the gamete formation by

Table 2. Statistics of the modified Cramér-von Mises goodness-of-fit test for daily temperature (maximum, mean, and minimum air temperatures) and relative air humidity data (maximum, mean, and minimum relative air humidity) of the historical series from 2007 to 2018, in the municipality of Juazeiro, in the state of Bahia, Brazil.

Modified Cramér-von Mises statistics-W*												
Month	Tmean				Tmax				Tmin			
	N	LN	G	GEV	N	LN	G	GEV	N	LN	G	GEV
Jan.	0.22	0.35	0.31	-	0.41	0.67	0.57	0.15	0.04	0.04	0.04	0.17
Feb.	0.15	0.26	0.22	-	0.83	1.21	1.07	0.41	0.06	0.03	0.04	0.04
Mar.	0.14	0.22	0.19	-	0.57	0.79	0.71	0.35	0.06	0.04	0.04	0.10
Apr.	0.07	0.10	0.09	-	0.43	0.68	0.59	0.09	0.10	0.17	0.14	0.19
May	0.08	0.10	0.09	-	0.15	0.25	0.21	0.09	0.41	0.63	0.55	0.39
June	0.11	0.06	0.08	-	0.04	0.03	0.03	0.06	0.21	0.35	0.30	0.09
July	0.13	0.20	0.17	-	0.11	0.19	0.16	0.23	0.19	0.39	0.32	0.12
Aug.	0.05	0.09	0.07	0.03	0.06	0.13	0.10	0.15	0.12	0.28	0.22	0.15
Sept.	0.08	0.14	0.12	0.02	0.16	0.28	0.23	0.16	0.06	0.07	0.06	-
Oct.	0.37	0.53	0.47	-	0.81	1.14	1.02	0.65	0.08	0.14	0.12	0.04
Nov.	0.43	0.61	0.55	-	0.76	1.12	0.99	0.46	0.03	0.06	0.05	0.06
Dec.	0.52	0.76	0.67	0.37	0.88	1.29	1.14	0.39	0.11	0.15	0.13	0.22
Month	Hmean				Hmax				Hmin			
	N	LN	G	GEV	N	LN	G	GEV	N	LN	G	GEV
Jan.	0.52	0.52	0.39	0.41	0.92	2.91	2.04	1.10	1.16	0.18	0.39	0.06
Feb.	0.62	0.22	0.32	-	0.40	0.46	0.42	0.52	0.81	0.11	0.26	0.03
Mar.	0.77	0.63	0.65	-	1.12	1.13	1.11	1.22	0.49	0.04	0.11	0.04
Apr.	0.65	0.30	0.38	0.24	0.76	0.56	0.61	1.04	1.94	0.30	0.67	0.09
May	0.35	0.12	0.16	0.14	0.56	0.36	0.42	0.39	0.23	0.04	0.04	0.03
June	1.25	0.67	0.84	0.13	0.56	0.33	0.40	0.18	0.41	0.09	0.15	0.10
July	1.11	0.56	0.72	0.17	0.61	0.36	0.44	0.18	0.34	0.05	0.09	0.06
Aug.	0.89	0.47	0.60	0.43	0.97	0.63	0.74	0.20	0.35	0.03	0.07	0.03
Sept.	0.65	0.31	0.41	0.23	1.17	0.80	0.91	0.21	0.76	0.38	0.40	0.39
Oct.	2.95	1.64	2.02	0.09	2.84	2.12	2.35	0.34	0.83	0.33	0.65	0.13
Nov.	0.90	0.44	0.57	0.10	1.11	0.74	0.85	0.31	0.67	0.24	0.27	0.26
Dec.	1.85	0.97	1.22	0.25	1.02	0.75	0.83	0.64	1.50	0.27	0.55	0.05

Probability distribution models: N, normal; LN, log-normal; G, gamma; and GEV, generalized extreme value. Tmin, minimum air temperature; Tmean, mean air temperature; Tmax, maximum air temperature; Hmin, minimum relative air humidity; Hmean, mean relative air humidity; and Hmax, maximum relative air humidity. (–) Represents the impossibility of estimating using the maximum likelihood method, due to the occurrence of a discontinuous region in the calculation of the number of derivatives during model adjustments.

reducing their quality, which leads to problems during fertilization, pollen germination, pollen tube growth, stigma receptivity, and the period of embryo formation and development (Hedhly, 2011).

El Yaacoubi et al. (2020) explained that environmental factors, especially the temperature-related ones, might lead to flowering changes and, consequently, induce erratic effects during fertilization. These effects might range from interrupting fertilization to degeneration of ovule development, externalized in physiological changes. High temperatures (32–34°C) during pollination were associated with embryo death after ovule fertilization and with deformed and seedless 'Irwin' mangoes (Kulkarni & Hamilton, 1993).

Tmean tends to be the hottest, in the last quarter of the year, with 40% (in 2 out of every 5 days from October to December) likelihood of temperatures being $\geq 28^\circ\text{C}$ (Figure 2 B). However, in the quarter from June to August, Tmean tends to be the coldest one, with temperature mean values lower than 28°C .

In a study on the effect of maximum and minimum daily temperatures on the seed and fruit developments of the mango cultivars 'Irwin', 'Kensington', and 'Nam Dok Mai' under controlled conditions, the authors observed that there was almost no incidence of stenospemocarpy after pollination in the group at 25/15°C treatment (Sukhvibul et al., 2005).

Hmean showed 99% probability of being equal to or higher than 50% in June (Figure 2 E). In this region,

Table 3. Statistics using the modified Anderson Darling goodness-of-fit test for daily temperature (maximum, mean, and minimum air temperatures) and relative humidity data (maximum, mean, and minimum relative air humidity) of the historical series from 2007 to 2018, in the municipality of Juazeiro, in the state of Bahia, Brazil.

Month	Modified Anderson-Darling statistics-A*											
	Tmean				Tmax				Tmin			
	N	LN	G	GEV	N	LN	G	GEV	N	LN	G	GEV
Jan.	1.47	2.26	1.98	-	2.65	4.22	3.65	0.94	0.34	0.33	0.31	1.11
Feb.	1.03	1.73	1.47	-	5.11	7.34	6.54	2.44	0.37	0.23	0.26	0.28
Mar.	0.94	1.44	1.25	-	3.57	4.87	4.41	2.24	0.37	0.29	0.29	0.63
Apr.	0.49	0.77	0.66	-	3.09	4.70	4.12	0.79	0.56	0.95	0.79	1.11
May	0.47	0.61	0.55	-	0.93	1.57	1.33	0.60	2.24	3.46	3.02	2.12
June	0.63	0.36	0.44	-	0.30	0.19	0.20	0.33	1.14	2.00	1.67	0.54
July	0.79	1.12	1.00	-	0.75	1.24	1.05	1.56	1.19	2.42	1.95	0.70
Aug.	0.36	0.62	0.51	0.18	0.46	0.98	0.77	1.12	0.84	1.82	1.44	1.08
Sept.	0.51	0.86	0.73	0.19	0.88	1.59	1.32	0.83	0.36	0.50	0.41	-
Oct.	2.56	3.54	3.19	-	5.21	7.19	6.48	4.21	0.46	0.82	0.67	0.24
Nov.	2.83	3.97	3.56	-	5.10	7.28	6.50	2.95	0.23	0.41	0.33	0.45
Dec.	3.17	4.58	4.07	2.22	5.29	7.67	6.83	2.27	0.63	0.86	0.76	1.24
Month	Modified Anderson-Darling statistics-A*											
	Hmean				Hmax				Hmin			
	N	LN	G	GEV	N	LN	G	GEV	N	LN	G	GEV
Jan.	3.35	4.93	3.55	3.17	8.68	21.8	16.24	6.48	7.27	1.30	2.63	0.52
Feb.	3.77	1.54	2.08	-	3.35	3.56	3.40	4.30	5.22	0.79	1.78	0.20
Mar.	4.78	3.68	3.88	-	7.34	7.28	7.24	8.16	2.95	0.29	0.68	0.29
Apr.	4.27	2.11	2.61	1.67	5.42	4.33	4.60	6.90	12.66	2.43	4.84	0.97
May	2.91	1.08	1.47	1.00	4.22	3.02	3.37	3.18	1.66	0.33	0.35	0.28
June	7.61	4.24	5.24	1.02	4.38	2.97	3.40	1.90	2.47	0.51	0.83	0.58
July	6.68	3.46	4.41	1.16	4.53	2.94	3.42	1.80	1.94	0.33	0.49	0.38
Aug.	5.24	2.92	3.59	2.73	6.28	4.23	4.86	1.63	2.11	0.28	0.47	0.29
Sept.	3.93	1.98	2.52	1.58	6.96	4.78	5.45	1.45	4.69	2.24	2.44	2.32
Oct.	17.3	9.80	12.0	0.59	15.7	11.68	12.0	2.08	6.09	2.18	4.23	0.89
Nov.	5.15	2.44	3.20	0.57	6.46	4.44	5.05	2.20	4.23	1.57	1.76	1.63
Dec.	10.9	5.84	7.27	1.67	6.93	5.30	5.75	4.61	9.41	1.74	3.55	0.33

Probability distribution models: N, normal; LN, log-normal; G, gamma; and GEV, generalized extreme value. Tmin, minimum air temperature; Tmean, mean air temperature; Tmax, maximum air temperature; Hmin, minimum relative air humidity; Hmean, mean relative air humidity; and Hmax, maximum relative air humidity. (–) Represents the impossibility of determining because the parameter estimates of the corresponding probabilistic model were not obtained using the maximum likelihood method.

spontaneous mango flowering begins during June (Mouco & Albuquerque, 2005), suggesting that this humidity level and the T_{mean} of $<28^{\circ}\text{C}$ are ideal for flowering mangoes in the study region. In general, there is an increasing probability of the mean humidity being equal to or higher than 70%, from December to April, with a maximum probability value of 29% expected for April. This trend is explained by the fact that the rainy season occurs in April, in this region.

In November, the expected daily T_{min} had a 67% probability of being higher than or equal to 22°C (Figure 2 C). Conversely, July and August had the

highest probability (75%) of $16\text{--}20^{\circ}\text{C}$ T_{min} . This temperature interval seems to be the most suitable for flowering, coinciding with the spontaneous bloom of mango trees in the region.

Low temperatures (mean temperatures of 14.8°C and minimum temperatures of 9.4°C) dramatically affected pollen production and development, according to the report by Lora & Hormaza (2018). Pollen had an irregular shape and altered the cell wall composition. Moreover, the vulnerability of gametophytes and sporophytes to low temperatures has been observed.

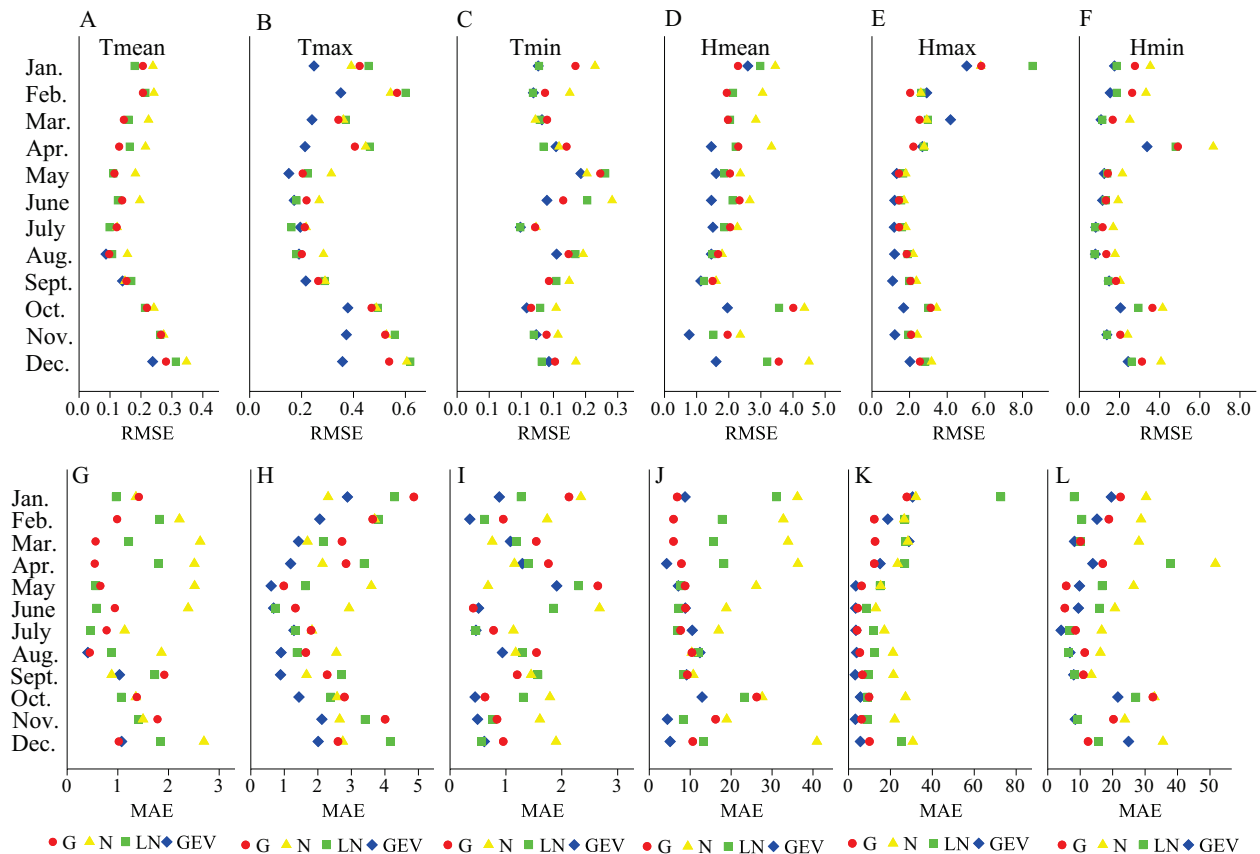


Figure 1. Root mean squared error (RMSE) of gamma (G), normal (N), log-normal (LN), and generalized extreme value (GEV) distributions regarding the following parameters: A, mean air temperature; B, maximum air temperature; C, minimum air temperature; D, mean relative air humidity; E, maximum relative air humidity; and F, minimum relative air humidity. MAE represents the absolute maximum error of the probability distributions (gamma, normal, log-normal, and generalized extreme value) regarding the following parameters: G, mean air temperature (T_{mean}); H, maximum air temperature (T_{max}); I, minimum air temperature (T_{min}); J, mean relative air humidity (H_{mean}); K, maximum relative air humidity (H_{max}); and L, minimum relative air humidity (H_{min}) of the historical series from 2007 to 2018, in the municipality of Juazeiro, in the state of Bahia, Brazil.

The price of 'Palmer' mango is correlated with the high levels of temperature and low levels of relative humidity (Figure 3). The highest prices per kilogram of 'Palmer' mango are generally paid five or six months

after the observed peaks of Tmax (Figure 3 A) and the lowest points of the Hmin curve (Figure 3 B).

Considering the price five months after the occurrence of each Tmax, the correlation between price and Tmax

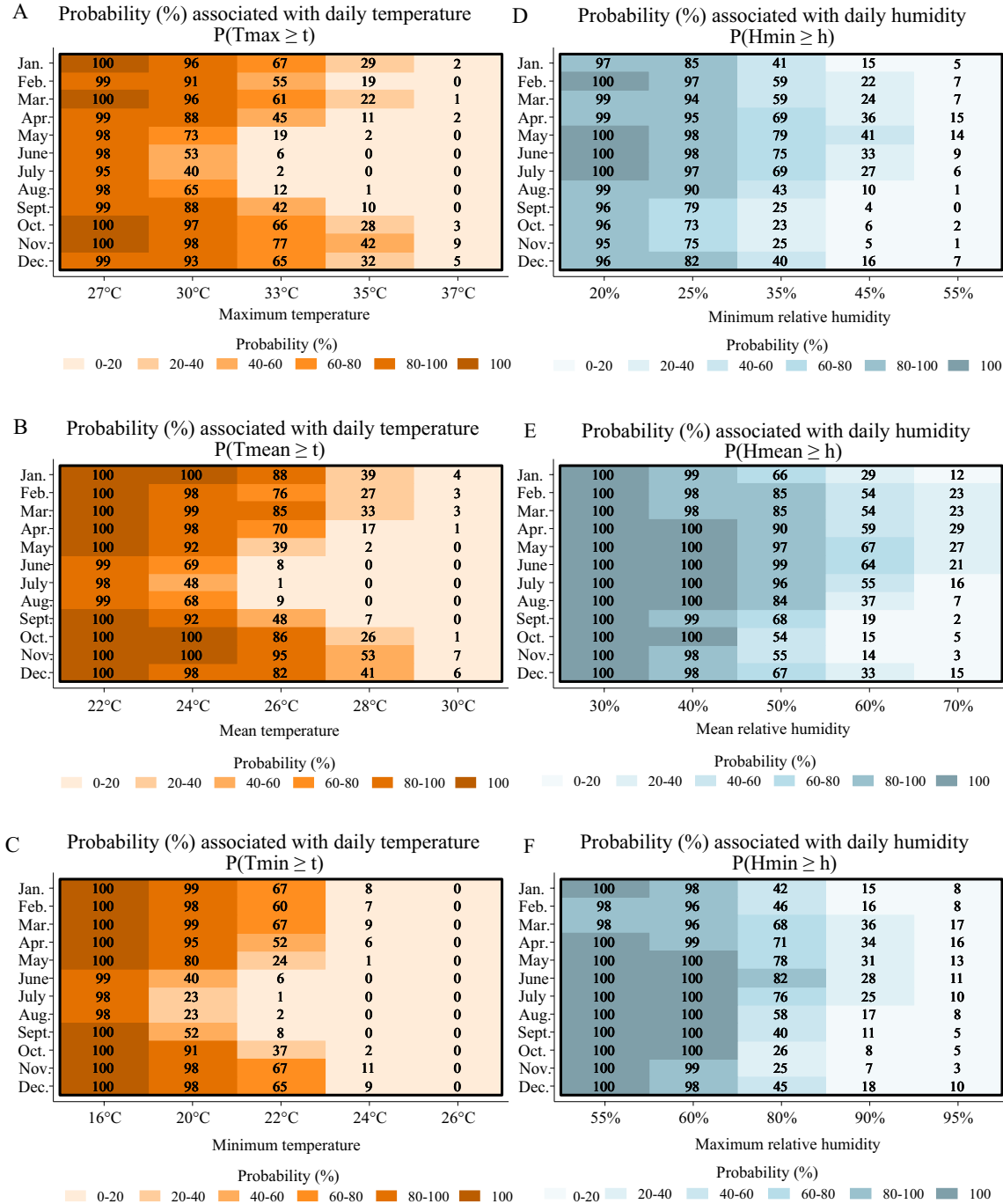


Figure 2. Probability estimates associated with different levels of air temperature and air humidity: A, maximum air temperature (Tmax); B, mean air temperature (Tmean); and C, minimum air temperature (Tmin); D, minimum relative air humidity (Hmin); E, mean relative air humidity (Hmean); and F, maximum relative air humidity (Hmax) of the historical series from 2007 to 2018, in the municipality of Juazeiro, in the state of Bahia, Brazil.

was 0.49. This is a strong and significant correlation ($p < 0.0001$). In contrast, Hmin had a weak (-0.11) and nonsignificant correlation under the same conditions. When a gap of six months was considered, the correlations of Tmax and Hmin were 0.34 ($p = 0.0041$) and -0.29 ($p = 0.014$), suggesting that both were significant. These results confirm that Tmax and Hmin ultimately affect the commercial value of 'Palmer' mangoes, as this variety has a long production cycle, taking on average five to six months from flowering to harvest.

High temperatures usually correlated with low relative air humidity might lead to the dryness of the stigma surface, thus not allowing of the pollen germination, which reduces yield and profit. França et al. (2010) explained that very dry pollen might have decreasing germination ability as it loses water content. This fact

directly affects fruiting and commercialization and, as a result, a lower number of fruit is formed and offered, which leads to the increase of demand and to a natural valuing of commercialized products.

These results show that the higher prices of 'Palmer' mango result from the higher incidence of stenospermocarpic fruit, due to their vulnerability to high temperatures and low relative humidity that occur during flowering or early fruit set. These occurrences directly affect fruit set and marketing, since, under adverse weather conditions, fewer fruit are formed and offered, which leads to the increase of demand and, consequently, to the increased appreciation of the products when marketed.

The joint probability level curves associated with Tmax and Hmin, based on the Frank copula density

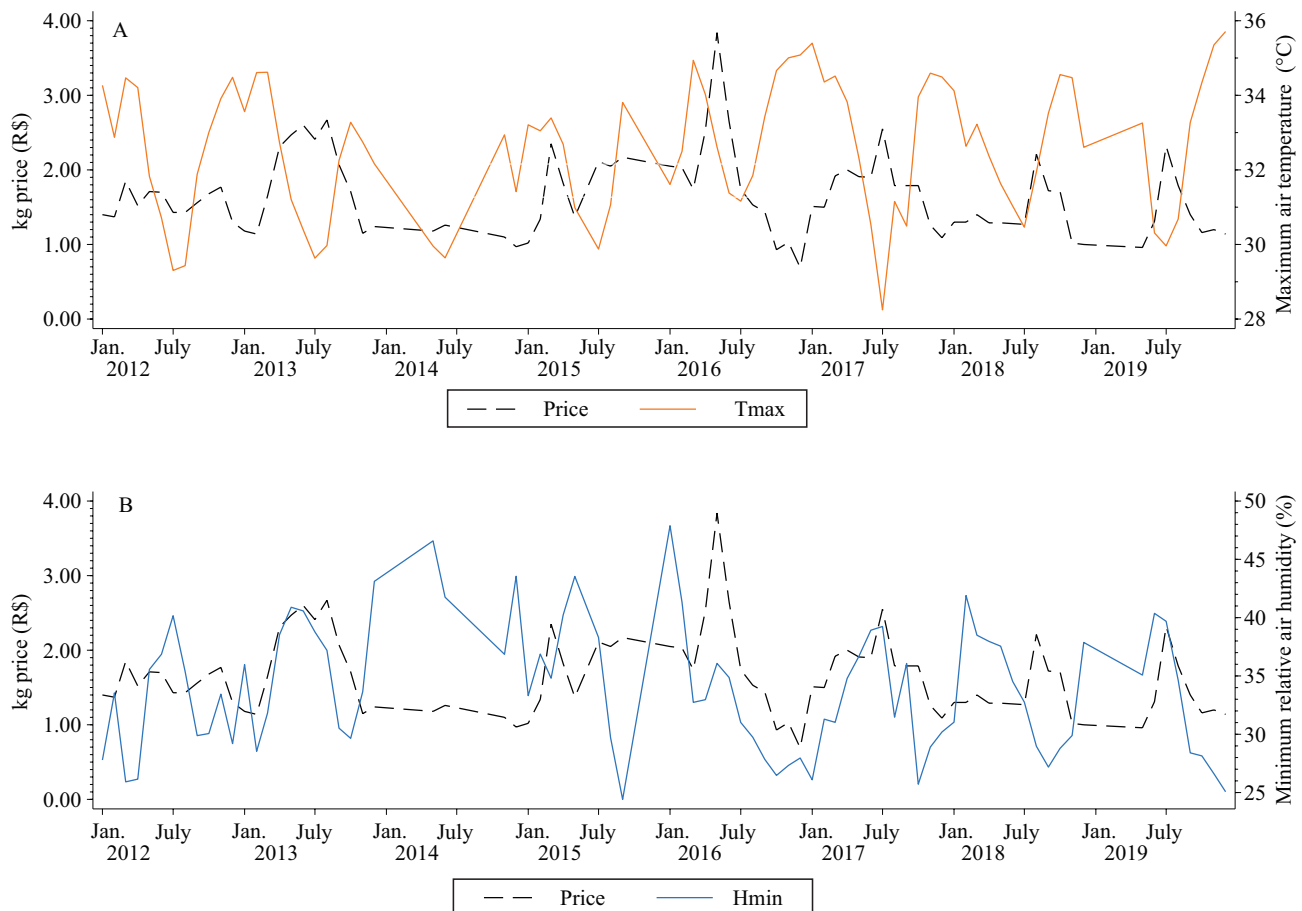


Figure 3. Price series (2012-2019) of 'Palmer' mango (*Mangifera indica*) commercialized in the Central Estadual de Abastecimento (CEASA), the state supply center of Bahia state, in Juazeiro, BA, Brazil, associated with fluctuations of maximum temperature (A) and minimum relative air humidity (B). Prices were obtained in the municipal supply service of Juazeiro, BA, and updated by IPCA (IBGE, 2024), according to the inflation in February 2020.

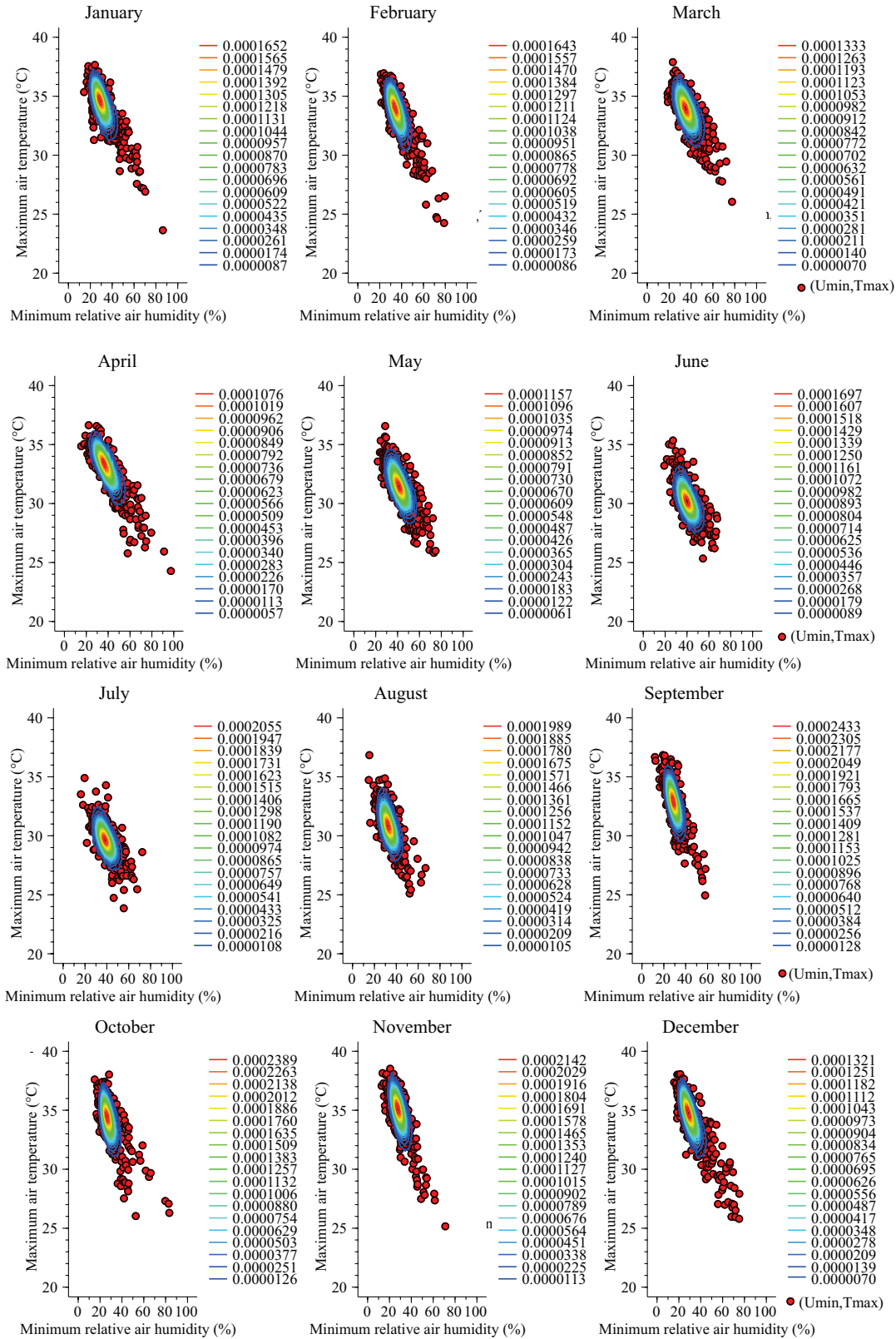


Figure 4. Dispersion graph of maximum temperature and minimum relative air humidity overlapped with the Frank copula probability density function associated with these joint variables of the historical series from 2007 to 2018, in the municipality of Juazeiro, in the state of Bahia, Brazil.

function, show a good fit to the data in each month (Figure 4).

Although it is not a copula with extreme values, its fitness to model the bidimensional dataset is possibly due to the good fit of generalized extreme value distribution, indicated by the KS adherence test and by W^* and A^* statistics. This shows that Frank copula goodness-of-fit test, with marginal GEV distributions, can be used to analyze joint Tmax and Hmin.

The excellent fit given to Frank copula in all months shows that it was able to absorb and model the dependence between maximum temperature and minimum relative humidity (Figure 4). Cai et al. (2019) evaluated the suitability of winter tourism, considering indices that include maximum temperature and relative air humidity. Comparing the Clayton, Gumbel, and Frank copulas functions, they found that Frank Copula was the most suitable to model these variables, as it obtained the lowest RMSE values.

The unimodality of the bivariate Frank copula probability density function is visually observable (Figure 4), with centered maximum probabilities indicated by a more intense red coloration. A dislocation of maximum probabilities is also visible, associated with a gradual increase of Tmax and a decrease of Hmin from 30°C and 40% in June, to 35°C and 30%, respectively, in November. This behavior follows the climatology of the study site, representing the dry season in this region, which might end with the first rains in November, according to Santiago et al. (2017).

It is worth noting that the Frank copula is symmetric and exhibits equivalent dependence patterns in both the upper and lower tails. However, when compared to a Gaussian copula, for instance, it has weaker tail dependence. When modeling two random variables via the Frank copula, Weber & Titman (2018) observed that they are positively associated when $\alpha > 1$, negatively associated when $\alpha < 1$, and become independent when $\alpha \rightarrow 1$.

Estimates of the parameter that measures the dependence between Tmax and Hmin, in the Frank copula (α), from January to December were -0.627, -0.625, -0.640, -0.639, -0.622, -0.643, -0.658, -0.662, -0.646, -0.689, -0.664, and -0.606, respectively. These values show an inverse association between Tmax and Hmin, with the maximum association observed in October, and the minimum one, in May. These months

are at the end of the dry and rainy seasons in the study area, respectively.

Bivariate estimates of probabilities are presented as jointly associated with different levels of Tmax and Hmin (Figure 5). Regarding probability estimates via the copula, one in two days in November is expected to have the highest probability (50%) of Hmin lower than or equal to 30%, and Tmax higher than or equal to 33°C. These are atmospheric conditions with extremely damaging effects on soft structures, such as plant reproductive structures. Such temperatures and humidity, co-occurring with mango bloom, might critically compromise the pollen viability and lead to several levels of chromosomal irregularities and meiotic changes.

The highest points in the temperature oscillation curve, which represent 'Palmer' mango prices, are closely related to probabilities calculated by the copula for October and November (Figure 3 A). These two months have maximum chances of 17% and 22%, respectively, of experiencing days with Tmax equal to or higher than 35°C, and Hmin lower than or equal to 25% (Figure 5). Extreme conditions such as these have devastating effects on plant physiology, requiring adaptation mechanisms. Unfortunately, these are absent in cultivars such as 'Palmer' which was developed for climatic conditions different from this region.

From January to December, Tmax and Hmin values in 2019 were, respectively: (34.5, 29.3); (34.8, 36.6); (33.9, 38.4); (33.4, 40.0); (33.3, 35.1); (30.3, 40.4); (30, 39.7); (30.7, 34.6); (33.3, 28.4); (34.3, 28.1); (35.4, 26.6); and (35.7, 25.1). According to the Frank copula, the probabilities associated with these months were 21, 36, 29, 26, 17, 24, 29, 25, 24, 26, 20, and 14%, respectively. This finding shows that the obtained bivariate probabilistic estimates were assertive because Tmax and Hmin of 2019 occurred within the probabilistic range (Figure 5). It is important to mention that incorrect probabilistic estimates in probability are only consistent when an event estimated as certainly does not occur.

The estimated probabilities are useful for farmers to choose between taking the risk of synchronizing flowering with less favorable seasons, expecting a higher value of the product when marketed, or avoiding critical seasons by advancing or delaying flowering, being aware of the management and production constraints that may arise in these periods.

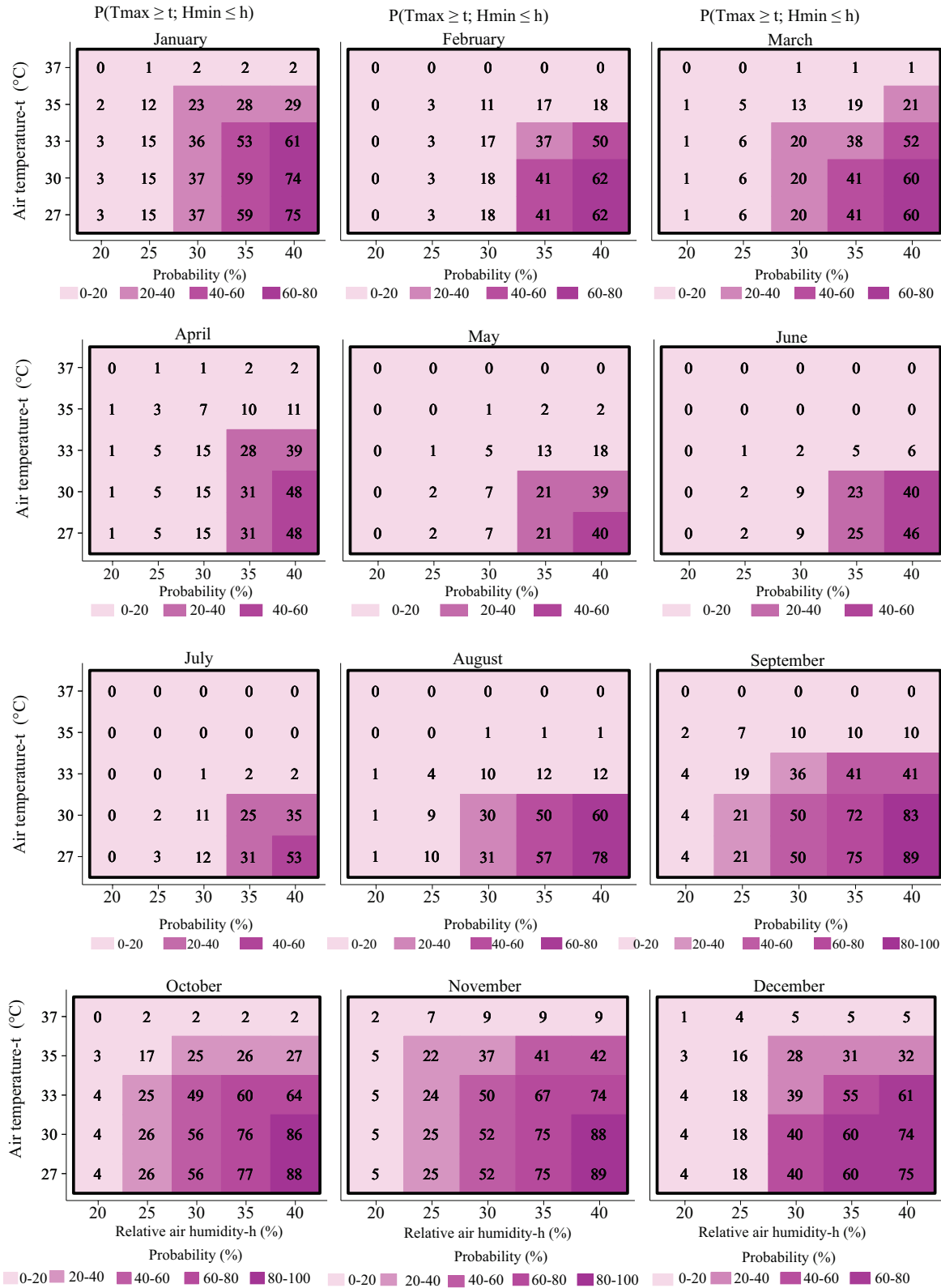


Figure 5. Joint probability of maximum air temperature (T_{max}) being equal to or greater than different levels of air temperature (t), and minimum relative air humidity (H_{min}) being less than or equal to different levels of relative air humidity (h) of the historical series from 2007 to 2018, in the municipality of Juazeiro, in the state of Bahia, Brazil.

Conclusions

1. November has a high probability of the simultaneous occurrence of high temperatures and low relative air humidity, making 'Palmer' mango (*Mangifera indica*) orchards in full bloom (or early fruiting) significantly subjected to extreme weather conditions, in the region of the Vale do Submédio São Francisco river, Brazil. These conditions are conducive to higher rates of stenopermocarpy in the harvests from April to May.

2. The Frank copula model is suitable for jointly modeling the maximum temperature and minimum relative humidity.

3. High temperatures and low relative air humidity significantly impact the prices of 'Palmer' mangoes, with periods of higher prices occurring six months after the peaks of high temperatures and the lowest indices of relative air humidity.

Acknowledgments

To Coordenação de Aperfeiçoamento de Pessoal de Nível Superior (CAPES), for funding in part this study (Code Finance 001).

References

- BACK, A.J.; CADORIN, S.B. Chuvas máximas diárias e equações intensidade-duração-frequência para o estado do Amapá, Brasil. **Revista Brasileira de Climatologia**, v.26, p.313-325, 2020. DOI: <https://doi.org/10.5380/abclima.v26i0.69844>.
- BADR, M.M. Goodness-of-fit tests for the compound Rayleigh distribution with application to real data. **Heliyon**, v.5, e02225, 2019. DOI: <https://doi.org/10.1016/j.heliyon.2019.e02225>.
- BELTRÁN, R.; VALLS, A.; CEBRIÁN, N.; ZORNOZA, C.; GARCÍA BREIJO, F.; REIG ARMIÑANA, J.; GARMENDIA, A.; MERLE, H. Effect of temperature on pollen germination for several Rosaceae species: influence of freezing conservation time on germination patterns. **PeerJ**, v.7, e8195, 2019. DOI: <https://doi.org/10.7717/peerj.8195>.
- CAI, W.; DI, H.; LIU, X. Estimation of the spatial suitability of winter tourism destinations based on copula functions. **International Journal of Environmental Research and Public Health**, v.16, art.186, 2019. DOI: <https://doi.org/10.3390/ijerph16020186>.
- CHEN, G.; BALAKRISHNAN, N. A general purpose approximate goodness-of-fit test. **Journal of Quality Technology**, v.27, p.154-161, 1995. DOI: <https://doi.org/10.1080/00224065.1995.11979578>.
- EL YAACOUBI, A.; EL JAOUHARI, N.; BOURIOUG, M.; EL YOUSSEFI, L.; CHERROUD, S.; BOUABID, R.; CHAOUI, M.; ABOUABDILLAH, A. Potential vulnerability of Moroccan apple orchard to climate change-induced phenological perturbations: effects on yields and fruit quality. **International Journal of Biometeorology**, v.64, p.377-387, 2020. DOI: <https://doi.org/10.1007/s00484-019-01821-y>.
- FRANÇA, L.V. de; NASCIMENTO, W.M.; CARMONA, R.; FREITAS, R.A. de. Tolerância à dessecação de pólen de berinjela. **Revista Brasileira de Sementes**, v.32, p.53-59, 2010. DOI: <https://doi.org/10.1590/S0101-31222010000100006>.
- HEDHLY, A. Sensitivity of flowering plant gametophytes to temperature fluctuations. **Environmental and Experimental Botany**, v.74, p.9-16, 2011. DOI: <https://doi.org/10.1016/j.envexpbot.2011.03.016>.
- HEIDE, O.M.; RIVERO, R.; SØNSTEBY, A. Temperature control of shoot growth and floral initiation in apple (*Malus domestica* Borkh.). **CABI Agriculture and Bioscience**, v.1, art.8, 2020. DOI: <https://doi.org/10.1186/s43170-020-00007-6>.
- IBGE. Instituto Brasileiro de Geografia e Estatística. **IPCA: Índice Nacional de Preços ao Consumidor Amplo: fevereiro 2020**. Available at: <https://www.ibge.gov.br/estatisticas/economicas/precos-e-custos/9256-indice-nacional-de-precos-ao-consumidor-amplio.html>. Accessed on: Apr. 24 2024.
- ISSARAKRAISILA, M.; CONSIDINE, J.A. Effects of Temperature on pollen viability in mango cv. 'Kensington'. **Annals of Botany**, v.73, p.231-240, 1994. DOI: <https://doi.org/10.1006/anbo.1994.1028>.
- KAYA, O.; ATES, F.; KARA, Z.; TURAN, M.; GUTIÉRREZ-GAMBOA, G. Study of primary and secondary metabolites of stenopermocarpic, parthenocarpic and seeded raisin varieties. **Horticulturae**, v.8, art.1030, 2022. DOI: <https://doi.org/10.3390/horticulturae8111030>.
- KRUEL, I.B.; MESCHIATTI, M.C.; BLAIN, G.C.; ÁVILA, A.M.H. de. Climate trends in the municipality of Pelotas, state of Rio Grande do Sul, Brazil. **Engenharia Agrícola**, v.35, p.769-777, 2015. DOI: <https://doi.org/10.1590/1809-4430-Eng.Agric.v35n4p769-777/2015>.
- KULKARNI, V.J.; HAMILTON, D. Fruit disorders in mango. In: NORTHERN TERRITORY. Department of Primary Industry and Fisheries. **Technical annual report 1992-93**. Berrimah: Department of Primary Industry and Fisheries, 1993. p.83-85. (Technical Bulletin, n.214). Available at: <https://territorystories.nt.gov.au/10070/687158/0/33>. Accessed on: Apr. 24 2024.
- LIU, X.; XIAO, Y.; ZI, J.; YAN, J.; LI, C.; DU, C.; WAN, J.; WU, H.; ZHENG, B.; WANG, S.; LIANG, Q. Differential effects of low and high temperature stress on pollen germination and tube length of mango (*Mangifera indica* L.) genotypes. **Scientific Reports**, v.13, art.611, 2023. DOI: <https://doi.org/10.1038/s41598-023-27917-5>.
- LORA, J.; HORMAZA, J.I. Pollen wall development in mango (*Mangifera indica* L., Anacardiaceae). **Plant Reproduction**, v.31, p.385-397, 2018. DOI: <https://doi.org/10.1007/s00497-018-0342-5>.
- MONTALT, R.; CUENCA J.; VIVES, M.C.; NAVARRO, L.; OLLITRAULT, P.; ALEZA, P. Influence of temperature on the progamic phase in *Citrus*. **Environmental and Experimental**

- Botany**, v.166, art.103806, 2019. DOI: <https://doi.org/10.1016/j.envexpbot.2019.103806>.
- MOUCO, M.A. do C.; ALBUQUERQUE, J.A.S. Efeito do paclobutrazol em duas épocas de produção da mangueira. **Bragantia**, v.64, p.219-225, 2005. DOI: <https://doi.org/10.1590/S0006-87052005000200008>.
- RAMÍREZ, F.; DAVENPORT, T.L. Mango (*Mangifera indica* L.) flowering physiology. **Scientia Horticulturae**, v.126, p.65-72, 2010. DOI: <https://doi.org/10.1016/j.scienta.2010.06.024>.
- REIS, C.J. dos; SOUZA, A.; GRAF, R.; KOSSOWSKI, T.M.; ABREU, M.C.; OLIVEIRA-JÚNIOR, J.F. de; FERNANDES, W.A. Modeling of the air temperature using the Extreme Value Theory for selected biomes in Mato Grosso do Sul (Brazil). **Stochastic Environmental Research and Risk Assessment**, v.36, p.3499-3516, 2022. DOI: <https://doi.org/10.1007/s00477-022-02206-1>.
- SANTIAGO, E.J.P.; OLIVEIRA, G.M.; LEITÃO, M.M.V.B.R.; MOURA, M.S.B.; GONÇALVES, I.S. Precipitação esperada, em diferentes níveis de probabilidade, na região de Juazeiro-BA. **Journal of Environmental Analysis and Progress**, v.2, p.457-464, 2017. DOI: <https://doi.org/10.24221/jeap.2.4.2017.1462.457-464>.
- SUKHVIBUL, N.; WHILEY, A.W.; SMITH M.K. Effect of temperature on seed and fruit development in three mango (*Mangifera indica* L.) cultivars. **Scientia Horticulturae**, v.105, p.467-474, 2005. DOI: <https://doi.org/10.1016/j.scienta.2005.02.007>.
- THINGREINGAM IRENAEUS, K.S.; MITRA, S.K. Understanding the pollen and ovule characters and fruit set of fruit crops in relation to temperature and genotype - a review. **Journal of Applied Botany and Food Quality**, v.87, p.157-167, 2014. DOI: <https://doi.org/10.5073/JABFQ.2014.087.023>.
- WANG, X.; ZANG, N.; LIANG, P.; CAI, Y.; LI, C.; YANG, Z. Identifying priority management intervals of discharge and TN/TP concentration with copula analysis for Miyun reservoir inflows, North China. **Science of the Total Environment**, v.609, p.1258-1269, 2017. DOI: <https://doi.org/10.1016/j.scitotenv.2017.07.135>.
- WEBER, E.M.; TITMAN, A.C. Quantifying the association between progression-free survival and overall survival in oncology trials using Kendall's τ . **Statistics in Medicine**, v.38, p.703-719, 2018. DOI: <https://doi.org/10.1002/sim.8001>.
- ZALINA, M.D.; DESA, M.N.M.; NGUYEN, V.-T.-V.; KASSIM, A.H.M. Selecting a probability distribution for extreme rainfall series in Malaysia. **Water Science and Technology**, v.45, p.63-68, 2002. DOI: <https://doi.org/10.2166/wst.2002.0028>.
-